Formulation of extrudable mortar

Rida Foulki [1*] , *Mouad* El Mesoudy[2], *Khalid* Cherkaoui[1] and *Driss* Amegouz[2]

[1]Department of Civil Engineering, ENSAM, Moulay Ismail University, Meknes, Morocco.
[2]2LTSI Laboratory, EST, Sidi Mohamed Ben Abdellah University, Fez, Morocco.

Abstract. The main objective of this study is to formulate an extrudable mortar. To achieve this goal, an experimental approach was adopted to optimize the mix design and improve the flow behavior of the fresh mortar, ensuring continuous and homogeneous extrusion. Several formulations were tested with a cylindrical extruder, varying the proportions of sand, fibers and superplasticizer. The study showed that fibers reduce flowability and increase water demand compared with non-fibrous mortars. Fibers also improve mix cohesion, which in turn improves mortar extrudability. Moreover, excessive sand content induces frictional behavior in the mix. Increasing the superplasticizer dosage from 1% to 3% allowed for a reduction in water content and enabled extrusion without water migration at low speed. Finally, extrusion speed was identified as a critical parameter for ensuring process success.

Keywords: Extruded mortar, Rheology, yield stress, Cement-based materials.

1 Introduction

Extrusion is a widely used forming process for viscoplastic materials, enabling specific shapes to be imparted by forcing them through a defined die. This process is particularly relevant for cementitious materials, such as mortars intended for 3D printing, requiring low yield stress for flow and sufficient yield stress post-deposition to maintain shape and support additional loads, such as the weight of top layers, as in the case of 3D printing of concrete by depositing successive layers.

In vertical extrusion, the tensile yield stress must exceed the gravitational stress to prevent filament rupture, and the material should resist phase migration and surface defects. Slow flow may induce fluid migration and increase apparent yield stress [1,2].
Extruders are generally categorized as ram or screw types, with screw extruders offering continuous extrudate. In piston extrusion, pressure rises with ram movement, stabilizes during flow, then spikes again as the die empties [3,4].

In this study, we investigate the effects of various mix design parameters on the extrudability of cementitious mortars, evaluating performance through pressure pro-files and visual assessment of extrudate quality.

* Corresponding author: r.foulki@edu.umi.ac.ma

2 Theoretical model

Analytical models have been developed to describe piston-driven extrusion of cementitious materials with complex viscoplastic behavior [5–8]. The rheology of fresh concrete is well captured by the Herschel–Bulkley model [9], which relates shear stress τ to shear rate $\dot{\gamma}$ as:

$$\begin{cases} \tau < \tau_0 : \dot{\gamma} = 0 \\ \tau \geq \tau_0 : \tau = \tau_0 + k(\dot{\gamma})^n \end{cases} \quad (1)$$

In this model, τ_0 denotes the yield stress, k represents the plastic viscosity, and n characterizes the flow behavior: shear-thickening when $n > 1$ and shear-thinning when $n < 1$. When $n = 1$, the Herschel–Bulkley model reduces to the linear form of the Bingham model [10].

The extrusion of fresh cementitious materials is effectively described by the uniaxial Herschel–Bulkley model, which captures axial deformation dominant in extrusion [11].

$$\sigma = \sigma_0 + k'(\dot{\varepsilon})^n \quad (2)$$

Where $\dot{\varepsilon}$ and σ represent the effective uniaxial strain rate and stress, respectively, and k' and σ_0 denote the flow consistency and uniaxial yield stress. Assuming isotropic flow behavior, Adams [12] established a relationship linking these uniaxial parameters to their corresponding shear values.

$$\tau_0 = \frac{\sigma_0}{\sqrt{3}} \quad ; \quad k = \frac{k'}{\sqrt{3}^{n+1}}$$

Basterfield et al. [13] developed a relationship between extrusion pressure and rheological parameters for an extruder with zero die length, under the assumptions of incompressibility, irrotational flow, and sufficiently slow flow to neglect inertia effects.

$$P_e = 2\sigma_0 \ln\left(\frac{D_0}{D}\right) + Ak'\left(\frac{2V_{out}}{D}\right)^n \left(1 - \left(\frac{D}{D_0}\right)^{3n}\right) \quad (3)$$

With

$$A = \frac{2}{3n}\left(\sin(\theta_{max})(1 + \cos(\theta_{max}))\right)^n$$

Here, P_e is the extrusion pressure, V_{out} the die exit velocity, D_0 and D the barrel and orifice diameters, and θ_{max} the slip-plane cone angle. Eq. (3) shows that lower yield stress and viscosity facilitate material flow, thereby enhancing extrudability.

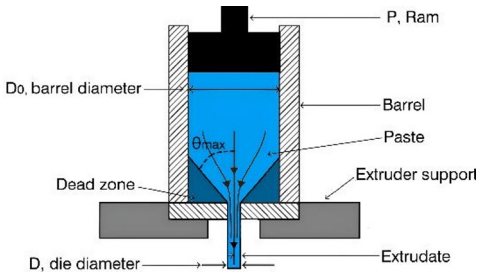

Fig. 1. Schematic of vertical ram extruder with typical flowlines.

Eq. (3) enables the estimation of rheological parameters of extrudable concrete via the ram extrusion method, which has been widely used to characterize cementitious materials [5–7,14]. In this approach, the material is extruded at various piston speeds, and steady-state pressure–velocity data are used to derive flow curves. The uniaxial yield stress can be obtained as die speed approaches zero.

At low extrusion speeds, water migration (drainage) may occur, affecting flow behavior. To address this, Martin et al. [15] proposed a criterion based on Terzaghi's consolidation theory to predict whether the mix remains homogeneous during extrusion:

$$t_{ext} < 0.1\frac{{H_d}^2}{C_v}$$

Where t_{ext} represents the extrusion time, C_v the consolidation coefficient and H_d the maximum drainage length.

3 Materials and methods

The cement used is CPJ 45, produced by Lafarge-Holcim and compliant with Moroccan standard NM 10.1.005 [16]. The superplasticizer is Viscocrete Tempo-10 M, an acrylic copolymer-based, non-chlorinated, high-range water reducer. Silica sand (CV 32) from Sibelco, representing the largest aggregate size in the studied formulations. The chemical composition of the cement and sand is shown in Table 1. The proper-ties of the superplasticizer and polypropylene fibers are detailed in Tables 2 and 3, respectively.

Table 1. Chemical composition of cement and silica sand.

Chemical composition	Quantity (by mass%)	
	Cement	Sand
CaO	57.66	0.01
SiO_2	17.07	99.00
Al_2O_3	4.11	0.49
Fe_2O_3	2.57	0.02
SO_3	1.78	-
MgO	1	-
K_2O	0.35	0.34
TiO_2	0.21	0.01
Others	0.21	-
LOI	14.3	0.1
specific gravity	3.13	2.64

Table 2. Properties of Admixture

Property	Value
Solid Content	29 ± 1.5%
PH (T=24+C)	4.38
Density	1.06 ± 0.01
Chloride ion content	≤ 1 %

Table 3. Properties of fibers.

Property	Value
Length/ Diameter	12 (mm)/ 30 (μm)
Density	0.91
Tensile strength	270-430 (Mpa)
Young's modulus in tensile	3000-6000 (Mpa)

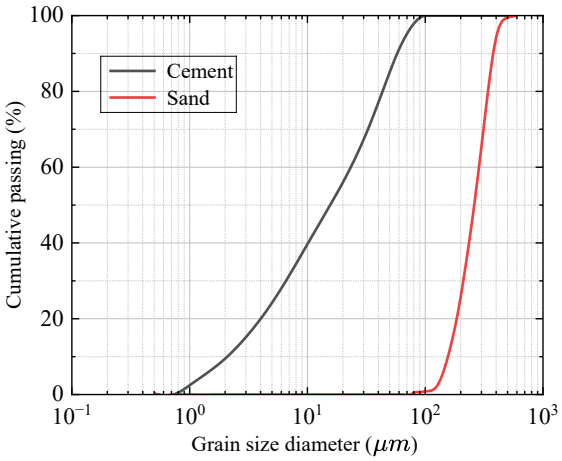

Fig. 2. Particle size distributions of the materials.

3.1 Mixtures proportions

Water content and superplasticizer dosage are key parameters in mix design, as they significantly influence the workability and rheological properties of the mixture.

Table 4. Concrete Mixture Proportions.

Mixture ID	Cement (g)	Sand (g)	Water (g)	Admixture (%)	Fibers (g)	W/C
F1	600	600	170	1%	0	0.29
F2	600	600	108	3%	0	0.201
F3	600	450	100	3%	0	0.196
F4	600	300	95	3%	0	0.188
F5	600	600	108	3%	1	0.21
F6	600	600	108	3%	2	0.21
F7	600	600	108	3%	3	0.21
F8	600	450	105	3%	2	0.205

3.2 Mixing procedure

Mixing was performed using a planetary mixer in accordance with EN 196-1 [17]. Dry materials were blended for 1 minute, followed by gradual addition of pre-mixed water and superplasticizer. Mixing continued for 1 minute at low speed and 15 minutes at high speed to ensure uniform dispersion and homogeneity. The extended mixing time is due to the low water-to-cement (w/c) ratios in the studied formulations.

4 Experimental program

4.1 Extrusion test

Extrusion tests were performed using a cylindrical extruder with a 107 mm diameter barrel and a 21.4 mm diameter die. Pressure was applied via a SERCOMP7 hydraulic press. A lubricated glass plate, inclined at 45°, was positioned 150 mm below the nozzle to guide the extrudate (Fig. 3). The mortar was loaded into the barrel, pre-formed with a 200 N preload while the die remained closed, and extruded 5 minutes after mixing at various ram speeds. Pressure–time curves were captured under a constant loading rate of 5 MPa/s, with the ram's own weight deemed negligible. Extrusion quality was primarily assessed via visual inspection for surface voids and discontinuities.

Fig. 3. Experimental setup for concrete extrusion.

4.2 Flow test

The flowability of the mixtures was evaluated using the flow table test in accordance with ASTM C1437 [18], which serves as an indicator of mortar consistency and fluidity. The flow diameter was measured after 25 drops, immediately following mixing.

5 Results and discussions

5.1 Mortar spread

The results indicate that the addition of fibers progressively reduces the flowability of the material. The fiber-free mixture (F2) exhibits high flow, whereas increasing the fiber content (F5 to F7) leads to a significant reduction in flow. Furthermore, a com-parison between F2 and F1 reveals that increasing the superplasticizer dosage from 1% to 3% enhances flowability by approximately 3%, despite a 30.68% reduction in water content.

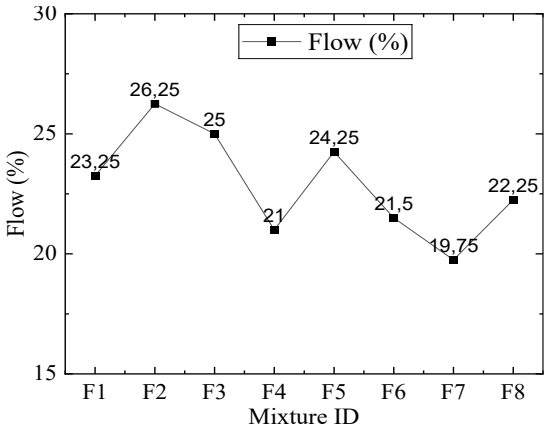

Fig. 4. Spreading test of mortars.

5.2 Admixture content effect

Comparison of F1 and F2 formulations highlights the effect of superplasticizer dos-age. At 10 mm/min, water drainage is observed with F1 but not with F2. However, for F1, this drainage does not occur when the extrusion speed is increased to 50 mm/min. These results suggest that both reducing the water content and increasing the extrusion speed can help prevent water migration. These findings justify the use of a high-range water reducer to enable stable extrusion, especially at low speeds.

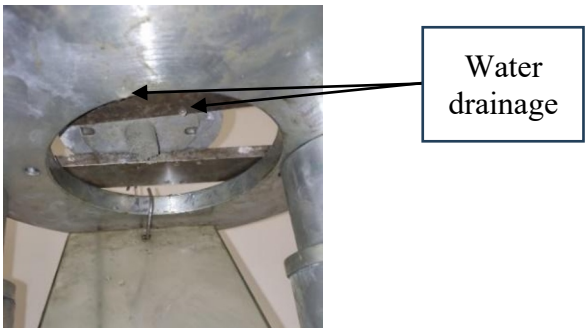

Fig. 5. Extrusion of F1 at speed of 10 mm/min.

5.3 Sand effect

Fig. 6 shows extruded samples that clearly demonstrate how reducing sand content affects extrudate quality. As expected, extrusion quality follows a clear trend with sand content. A high sand content results in rough, cracked, and crumbly extrudates, indicating poor cohesion (F2). However, by progressively reducing the sand content, cracks are minimized, and the extrudates become more cohesive, homogeneous, and regular free from major surface defects (F3 to F4).

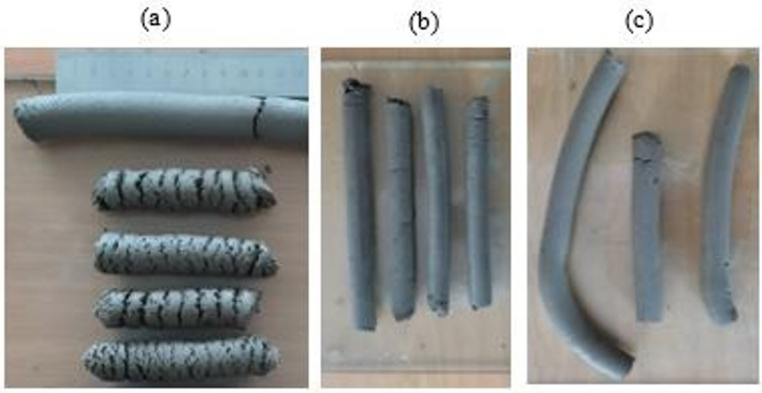

Fig. 6. Sand content effect on extrudate quality at 50 mm/min: (a) F2; (b) F3; (c) F4.

From Fig. 7, we can observe that the pressure required for extrusion increases with the sand content. Formulation F2, which contains the highest sand content, exhibits a highly irregular curve marked by fluctuations and perturbations throughout the extrusion process. These disturbances suggest poor cohesion and unstable flow. In contrast, formulations F3 and F4, with reduced sand content, display smoother and more stable pressure–time curves. This improved regularity reflects enhanced plasticity and internal cohesion.

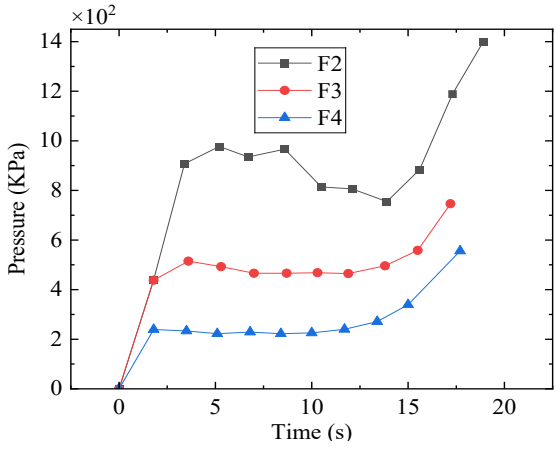

Fig. 7. Comparison of effort evolution over time for F2, F3 and F4 formulations.

5.4 Fibers effect

Fig. 8 shows that the gradual addition of fibers improves the ductility of extrudates. In the absence of fibers (F2), extrudates are rigid and brittle, while the introduction of fibers (F5) promotes more plastic behavior and better cohesion. However, a high dosage (F7) causes irregular deformations of the filament. As shown in Fig. 9, the addition of fibers reduces the extrusion pressure and enhances process stability. An optimal fiber content improves internal cohesion and reduces internal friction, promoting more uniform and continuous extrusion.

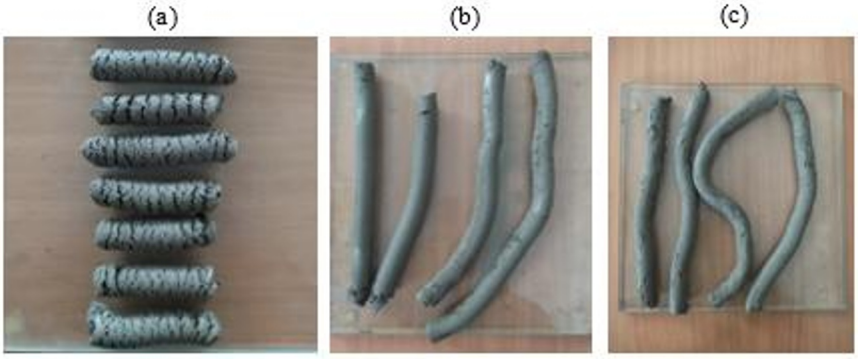

Fig. 8. Fibers content effect on extrudate quality at 100 mm/min: (a) F2; (b) F5; (c) F7.

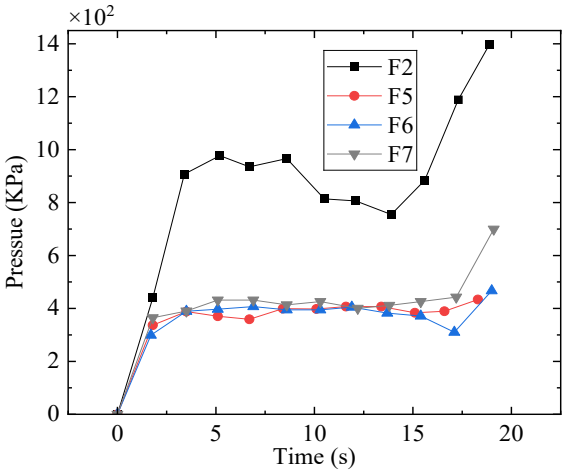

Fig. 9. Comparison of effort evolution over time for F2, F5, F6 and F7 formulations.

5.5 Extrudability results

Extrusion tests were carried out at two different ram speeds: 50 mm/min and 100 mm/min. All formulations were non-extrudable, except for F8, which was extrudable at both speeds, and F4, which was extrudable only at 100 mm/min (Fig. 10). The behavior of F4 extrudable at high speed but not at low speed can be explained by the fact that at 50 mm/min, the gravitational stress exerted by the material at the die acts for a longer duration (twice as long as at 100 mm/min).

Fig. 10. Extrudable formulations at 100mm/min: (a) F4; (b) F8.

6 Conclusion

This study developed and evaluated extrudable mortar formulations, with a focus on optimizing rheological properties critical to successful extrusion. The key findings are summarized as follows:

- The incorporation of fibers significantly reduced mortar flowability, increased water demand, and enhanced cohesion, thereby improving extrudability. However, excessive fiber content adversely affected the extrusion quality, emphasizing the necessity of an optimal fiber dosage.
- Adjustments in sand content had a pronounced impact on the extrusion quality and pressure required. High sand content led to increased friction, resulting in brittle, irregular extrudates. Reducing sand content improved cohesion, producing smoother and more homogeneous extrudates.
- Increasing the superplasticizer dosage from 1% to 3% notably improved the mix-ture's extrudability by preventing water drainage at low speed.
- The extrusion speed was confirmed as a critical process parameter.

Future work will aim to improve sustainability and cost-efficiency by optimizing the cement content through partial substitution with supplementary materials. The im-proved formulations will be evaluated in a 3D printing setup to assess pumpability and buildability under realistic deposition conditions.

Acknowledgments. The authors acknowledge the financial support of the Centre National pour la Recherche Scientifique et Technique (CNRST) for this work within the framework of the Bourse Pass program.

Disclosure of Interests. The authors declare no competing interests.

References

1. Toutou, Z., Roussel, N., Lanos, C.: The squeezing test: a tool to identify firm cement-based material's rheological behaviour and evaluate their extrusion ability. Cement

Concr. Res. 35(10), 1891–1899 (2005). https://doi.org/10.1016/j.cemconres.2004.09.007

2. Perrot, A., Mélange, Y., Rangeard, D., Estellé, P., Lanos, C.: Extrusion criterion for firm cement-based materials. In: AIP Conference Proceedings, vol. 1, pp. 96–98. AIP, (2008). https://doi.org/10.1063/1.2964911
3. Liu, H., Liu, J., Leu, M.C., Landers, R., Huang, T.: Factors influencing paste extrusion pressure and liquid content of extrudate in freeze-form extrusion fabrication. Int. J. Adv. Manuf. Technol. 67, 899–906 (2012). https://doi.org/10.1007/s00170-012-4534-0
4. Mounanga, P., Cherkaoui, K., Khelidj, A., Courtial, M., de Noirfontaine, M.-N., Dunstetter, F.: Extrudable reactive powder concretes hydration, shrinkage and transfer properties. Eur. J. Environ. Civ. Eng. 16, 99–114 (2012). https://doi.org/10.1080/19648189.2012.681961
5. Li, Z., Zhang, Y., Zhou, X.: Short fiber reinforced geopolymer composites manufactured by extrusion. J. Mater. Civ. Eng. 17(6), 624–631 (2005). https://doi.org/10.1061/(ASCE)0899-1561(2005)17:6(624)
6. Zhou, X., Li, Z.: Characterization of rheology of fresh fiber reinforced cementitious composites through ram extrusion. Mater. Struct. 38(1), 17–24 (2005). https://doi.org/10.1007/BF02480570
7. Alfani, R., Grizzuti, N., Guerrini, G.L., Lezzi, G.: The use of the capillary rheometer for the rheological evaluation of extrudable cement-based materials. Rheol. Acta 46(5), 703–709 (2007). https://doi.org/10.1007/s00397-007-0164-0
8. Zhou, X., Li, Z., Fan, M., Chen, H.: Rheology of semi-solid fresh cement pastes and mortars in orifice extrusion. Cement Concr. Compos. 37, 304–311 (2013). https://doi.org/10.1016/j.cemconcomp.2013.01.004
9. Herschel, W.H., Bulkley, R.: Konsistenzmessungen von Gummi-Benzollosungen. Kolloid-Z. 39, 291–300 (1926). https://doi.org/10.1007/BF01432034
10. Bingham, E.C.: Fluidity and Plasticity. 2nd edn. McGraw-Hill, New York (1922)
11. Basterfield, R.A., Lawrence, C.J., Adams, M.J.: On the interpretation of orifice extrusion data for viscoplastic materials. Chem. Eng. Sci. https://doi.org/10.1016/j.ces.2004.12.019
12. Adams, M.J., Aydin, I., Briscoe, B.J., Sinha, S.K.: A finite element analysis of the squeeze flow of an elasto-plastic paste material. J. Non-Newtonian Fluid Mech. 71, 41–57 (1997). https://doi.org/10.1016/S0377-0257(96)01546-7
13. Basterfield, R.A., Lawrence, C.J., Adams, M.J.: On the interpretation of orifice extrusion data for viscoplastic materials. Chem. Eng. Sci. https://doi.org/10.1016/j.ces.2004.12.019
14. Perrot, A., Mélange, Y., Rangeard, D., Micaelli, F., Estellé, P., Lanos, C.: Use of ram extruder as a combined rheo-tribometer to study the behaviour of high yield stress fluids at low strain rate. Rheol. Acta 51(8), 743–754 (2012). https://doi.org/10.1007/s00397-012-0638-6
15. Martin, P.J., Wilson, D.I., Bonnett, P.E.: Paste extrusion through non-axisymmetric geometries: insights gained by application of a liquid phase drainage criterion. Powder Technol. 168, 64–73 (2006). https://doi.org/10.1016/j.powtec.2006.06.018
16. IMANOR: NM 10.1.005: Liants Hydrauliques – Techniques des essais. Norme Marocaine, (2008)
17. AENOR: EN 196-1:2005: Methods of Testing Cement – Part 1: Determination of Strength. AENOR, Spain (2005)

18. ASTM C1437-15: Standard Test Method for Flow of Hydraulic Cement Mortar. ASTM International, West Conshohocken, PA (2015)